NASA CR- N76-25315

CR-144756

PRELIMINARY ANALYSIS OF 15 GHz SCINTILLATIONS ON AN ATS-5 SATELLITE-TO-GROUND PATH

C. A. Levis and V. Ungvichian

The Ohio State University

ElectroScience Laboratory

Department of Electrical Engineering
Columbus, Ohio 43212

ITEM II FINAL REPORT
Report 3863-7

February 1976

NATIONAL AERONAUTICS & SPACE ADMINISTRATION
Goddard Space Flight Center
Greenbelt Road
Greenbelt, Maryland 20771

NOTICES

TECHNICAL REPORT STANDARD TITLE PAGE

1. Report No.	2. Government Accession No.	3. Recipient's Catalog No.
4. Title and Subtitle PRELIMINARY ANALYSIS OF 15 GHz SCINTILLATIONS ON AN ATS-5 SATELLITE-TO-GROUND PATH		5. Report Date February 1976 6. Performing Organization Code ESL 3863-7
7. Author(s) C. A. Levis and V. Ungvichian		8. Performing Organization Report No.
9. Performing Organization Name and Address The Ohio State University ElectroScience Laboratory, Department of Electrical Engineering, Columbus, Ohio 43212		10. Work Unit No. NAS5-21983 11. Contract or Grant No. NAS5-21983
12. Sponsoring Agency Name and Address NASA, GSFC Greenbelt, Maryland 20771 E. Hirschmann, Code 951, Technical Officer		13. Type of Report and Period Covered Item II Final Report 6/11/74 - 1/31/76 14. Sponsoring Agency Code 60
15. Supplementary Notes		

16. Abstract

Although the ATS-5 satellite failed to de-spin, a rather intricate analysis procedure allows the extraction of scintillation information at spectral rates from 20 to 60 Hz, as well as below 0.5 Hz. The procedure has been applied to 15.3 GHz signals received at Columbus, Ohio. Distributions and spectra were obtained for a limited amount of data, representing a variety of meteorological conditions. A definite correlation of scintillation strength and variability with rainfall is apparent. The data analysis is continuing.

17. Key Words (Selected by Author(s))	18. Distribution Statement		
Scintillation Propagation Satellite Communications Millimeter Waves Centimeter Waves			
19. Security Classif. (of this report) U	20. Security Classif. (of this page) U	21. No. of Pages 23	22. Price*

*For sale by the Clearinghouse for Federal Scientific and Technical Information, Springfield, Virginia 22151.

PREFACE

The objective of this research is to obtain scintillation information from data obtained in 1969-1971. Such an analysis had been intended prior to the ATS-5 launch, but it was abandoned when the satellite failed to despin. The analysis described in this report shows how the spin effects may be removed from the data to give information at both slow and fast scintillation rates. No information was recovered in the intermediate range. Both slow and fast scintillations are present at all times; they increase in magnitude and variability under conditions of light and hard rainfall. These results are based on the analysis of only a small amount of data; it is anticipated that the computer programs available as a result of this work will be used to analyze further data, which has already been digitized, in order to support and extend the results given here.

CONTENTS

I. INTRODUCTION

The ATS-5 Satellite was launched in August 1969, and its 15.3 GHz down-link signal was received at The Ohio State University between 25 November 1969 and 20 September 1971. Although the satellite was designed to be despun and gravity-gradient stabilized, this maneuver was prevented by problems during the insertion of the satellite into orbit. As a result, it remained spinning at approximately 76 rpm, with its spin axis inclined approximately 2° with respect to that of the Earth. [1]

The spin causes the beam of the satellite antenna to sweep across receiving stations on the Earth. Therefore the transmissions from the satellite, which are themselves not modulated, are received as a series of pulses, one every 1/76 minute or 789 milliseconds, as shown in Fig. 1. Each pulse is a "cut" through the antenna pattern of the satellite antenna. The peak of each received pulse occurs when the satellite antenna is pointed most nearly at the receiving station. Because of the inclination of the satellite spin axis with respect to that of the Earth and, to a lesser extent, because the orbital plane is inclined slightly with respect to the Earth's equatorial plane, the pattern changes diurnally. Figure 2a shows the configuration when the beam is directed maximally toward the North. The situation 12 hours later is shown in Fig. 2b. During the intervening time, the Earth has rotated one-half revolution. The satellite, which is approximately geostationary, has revolved with the Earth, but the orientation of its spin axis in space remains unchanged; therefore the beam maximum is now directed more toward the South, illustrating the diurnal change (on an exaggerated scale). The resulting change in the peak signal received at Columbus, Ohio was approximately 3.4 decibels. Propagation and noise effects are superimposed on the rotational and diurnal signal variations. The objective is to separate out and assess the propagation effects, and in particular scintillation effects.

Previous analyses of the ATS-5 data have concentrated primarily on the statistical distribution of fading, the correlation between fading and radiometric observations, and the spatial correlation of fading at distances useful for diversity reception [1-5]. Scintillations have received less attention, partly because the systems implications of deep fading are of greater significance, and partly because the spin-modulation of the satellite signal makes scintillation studies difficult [6]. In 1972 Struharik and Levis proposed and demonstrated an analysis method for obtaining scintillation statistics for a spinning satellite [7]. The proposal was implemented in summer 1974, and the initial results of the analysis are reported here.

II. ANALYSIS METHOD

The spin-modulation of the signal may be interpreted as a sampling process in which the sampling waveform is a train of the satellite antenna patterns instead of the more usual rectangular pulse train. This sampling convolves the spectrum of the desired satellite signal with that of the sampling waveform. Complete extraction of the signal as it existed before this sampling is not possible by even the most sophisticated means; in any case, the volume of data available for analysis dictates a relatively simple approach.

The approach employed here utilizes an averaging process to obtain the current antenna pattern "cut", and then calculates how the actual pulses differ from this pattern replica. In this way, information is obtained in two spectral ranges. The first encompasses frequencies lower than half the sampling rate, i.e., the approximate range 0-0.5 Hz. The second encompasses a range such that a period is substantially smaller than the length of one sample pulse, but within the receiver passband, i.e., approximately 20-60 Hz. We shall refer to the first range as "slow" scintillations and the second as "fast" scintillations.

The steps in performing the analysis are shown in Fig. 3. In order to average the digitized pulses, they must first be lined up. This is accomplished by correlating each pulse with a half-sine wave of approximately the same shape as the pulse and storing the data in an array in the position of best correlation. In order to improve the correlation accuracy, the data points, which represent sampling at 4-millisecond intervals in real time, are interpolated to 1/2-millisecond intervals using fourth-order polynomials and Newton's method. The correlated pulses are next multiplied by a scale factor which equalizes their areas, and then they are averaged to obtain the desired pulse replica of the signal with noise and propagation effects averaged out. The replica is next rescaled to the same area as the interpolated data pulse and the two are subtracted. The resulting difference, shown on the bottom of Fig. 3, represents only noise in the time before and after each pulse, while during the pulse time it represents the effects of noise plus rapid scintillations. The latter turn out to predominate, as is apparent when the differences near the pulse center are compared with those before and after the pulse. The rms value of the difference in the central portion of the pulse is taken as a measure of fast scintillation strength. The time periods at the very beginning and end of each pulse are not used in the analysis because the receiver phase-lock loop lock-on and drop-out might produce errors and, in any case, the scintillation-to-noise ratio is low during these periods. The inverse of the scale factor used to normalize the pulse areas is a measure of the slow scintillations, or alternatively the average of a number of data points near the peak of the pulse may be used for this measure.

Figures. 4-6 indicate how well the correlation and averaging procedures work under various signal strength conditions. Each shows a few pulses in their correlated positions and also the shape of the replica pulse

which results from averaging 40 pulses, including those shown. Using a greater number of pulses in the averaging results in a smoother average pulse, but the assumption that the propagation process is stationary is not justified if too long a data time period is involved. The use of 40 samples, corresponding to 31.6 seconds of data time, appears to be a reasonable compromise.

A simple test can be used to see to what extent the difference values, obtained by subtracting the average pulse shape from the individual pulses, represent propagation effects as contrasted with noise and data-processing effects. This test is based on the fact that propagation effects are multiplicative; their magnitude is directly proportional to signal strength. This proportionality is explored in the top three traces of Fig. 7. For each trace, 40 pulses have been processed by obtaining the difference at 4-millisecond time intervals; the rms value of the 40 values for each such time is plotted in the figure. The strong correlation with signal strength, as indicated by the average pulse shown below the rms difference traces, supports the multiplicative nature of the effect. Also it should be noted that near the signal peak the rms difference exceeds the rms noise value, as recorded before and after the pulses, by about 10 dB. The dependence of the statistics on meteorological factors, discussed in the next section, also indicates that the analysis procedure does yield propagation effects.

III. RESULTS

The running time of the program, using our Datacraft 6024 processor, is approximately equal to the real time during which data was taken. Time sharing slows it down proportionately to the number of users. This means that data has to be selected judiciously for processing and that the analysis has to be stretched out over a substantial period of time in order to coordinate the analysis with other tasks which require use of the same processor. The preliminary data reported here is taken from analog tape 23, recorded on 15 June 1970. This tape was selected because of the variety of weather conditions represented during a single run: notations logged at the time of the observations include cloudy, hard rain, light rain, broken clouds/overcast, and clear sky.

The statistical distribution of the fast scintillations is shown in Fig. 8. Because of the multiplicative nature of propagation effects, the significant parameter is the ratio of the scintillations to the steady signal component; the scintillation values are therefore divided by the value obtained by averaging five sample values (spaced 4 milliseconds apart) about the pulse maximum, as indicated at the top right of the figure. The distribution is seen to be strongly dependent on precipitation, but fast scintillations were observed essentially all of the time. Under broken clouds/overcast conditions their median rms level was about 0.3 db, and 0.8 db was rarely exceeded. During heavy rain, the median level rose to about 0.6 db and 1.7 db was rarely exceeded, again on an rms basis.

The time-changing behavior of the fast scintillations is shown in the spectra of Figs. 9 and 10. It should be remembered that the fast scintillations represent signal variations at rates between approximately 20-60 Hz, the lower limit being fixed by the time duration of each spin-modulation pulse and the upper by the receiver bandpass. We are unable to resolve this spectral region in detail because of the spin-modulation sampling; instead, the fast scintillations during any one sample pulse have been lumped into a single rms value. Nevertheless one can ask on what slower time scale the fast scintillation statistics are varying. This question can be answered by treating each rms value, corresponding to the fast scintillations during one spin-modulation pulse, as a single sample value and taking the spectrum of the time sequence of such sample values. Figures 9 and 10 are such spectra. It is reasonable to assume that the original (20-60 Hz) spectra would relate to the microstructure of hydrosols and turbulence, while the spectra of Figs. 9 and 10 might relate to the mesostructure, on the scale perhaps of clouds, but a firm theoretical basis for this speculation seems to be lacking at present. Under clear-sky conditions, as in Fig. 9, the spectrum appears to be relatively flat and featureless between 0 and 0.3 Hz. The ordinate gives the values, on a voltage basis, relative to the steady component. If the rms value of the spectral components came to the dotted line, the steady and variable components would represent equal powers; it is therefore clear that under clear-sky conditions the fast scintillations were quite stable over the approximately 7-minute period represented in Fig. 9. In contrast, during hard rain, the variability increases considerably as shown by the spectrum of Fig. 10 and the "tail" of the distribution in Fig. 8. The first few large components in Fig. 10, representing periods of the order of one to a few minutes, are probably representative of the morphology of the rain storm and might be expected to vary considerably from storm to storm. The data processing of the spectrum for this initial data set was quite unsophisticated; no attempt was made to remove trends, check for stationarity, average many spectra, or estimate confidence limits.

The cumulative distribution of slow scintillations is shown in Fig. 11. It is seen that rain reduces the amplitude of the average signal, as is well known. Rain also increases the signal variability considerably. The corresponding spectrum for hard rain appears in Fig. 12. The components with periods on the order of a minute correlate reasonably well with those of the fast scintillations for the same time interval, which supports the assumption that these represent the morphology of the rain storm. Under broken-cloud and clear-sky conditions, the slow scintillations are quite small and relatively featureless, as shown in Fig. 13.

Data pulses with unusual properties are occasionally detected during the correlation process. One example, a pulse of greatly reduced amplitude, is evident in Fig. 14. Another, a pulse of greatly reduced width (fifth from bottom), appears in Fig. 15. It should be noted that the time elapsed between each pulse and the one shown above and below it is only 0.789 seconds. The cause of the anomalies is not known.

IV. CONCLUSIONS

The processing scheme proposed for scintillation analysis of ATS-5 data has been implemented and works satisfactorily. Even under clear-sky conditions, fast scintillations can be sensed with about 10 db margin above the system and quantization noise. The processing time on the Datacraft 6024 processor is approximately equal to the real time of the observations. A strong correlation with rain is observed for both fast and slow scintillations. The time variations of the phenomena responsible for both slow and fast scintillations give rather featureless spectra in the region 0-0.3 Hz, except for very slow components which probably reflect the gross morphology of the storm.

V. PLANS FOR THE FUTURE

We plan to analyze sufficient segments of the digitized data (listed in Table A) to give statistically significant results for a variety of weather conditions. Because of the large amount of available data and relatively long processing time, this analysis will have to be spread over a period of several months in order to avoid overloading the processing system, which is shared with all other projects of the Laboratory. An alternative possibility to be explored is to have the analysis program run, at least in part, at Goddard Space Flight Center. A technical report on the entire data set is planned.

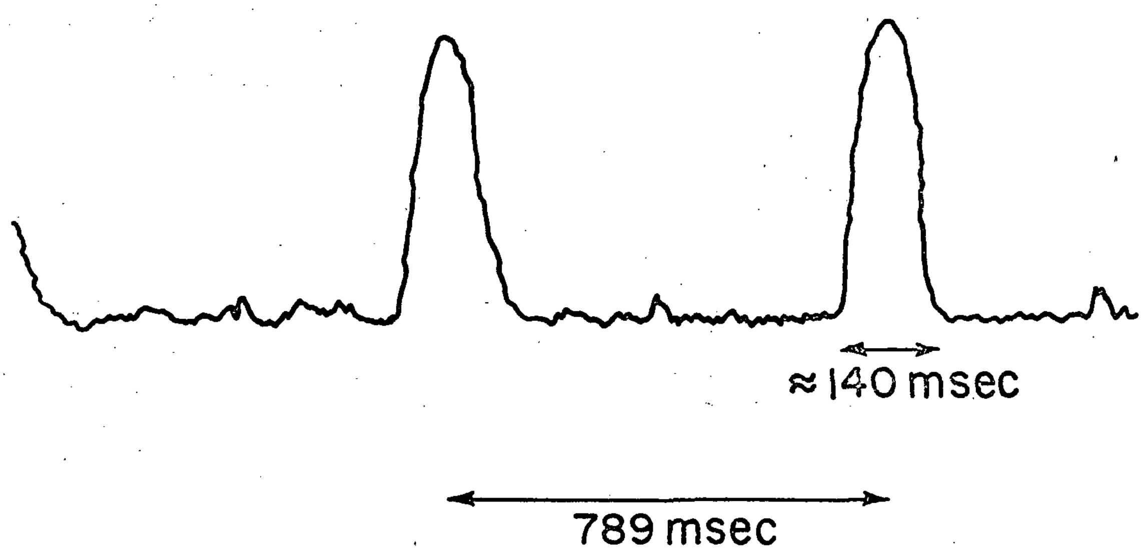

Fig. 1. Typical signal waveform.

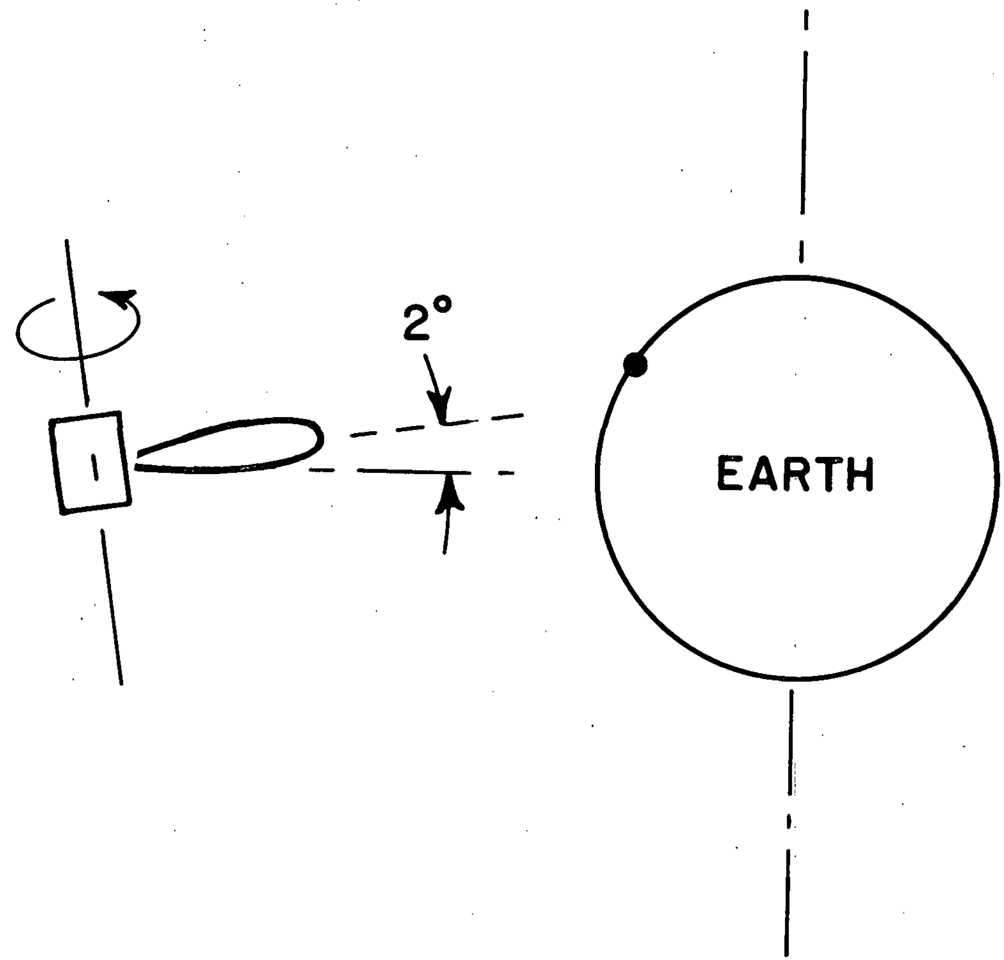

Fig. 2a. Spin modulation and its diurnal variation. (Scale distorted to exaggerate diurnal effects). Maximum northward beam excursion.

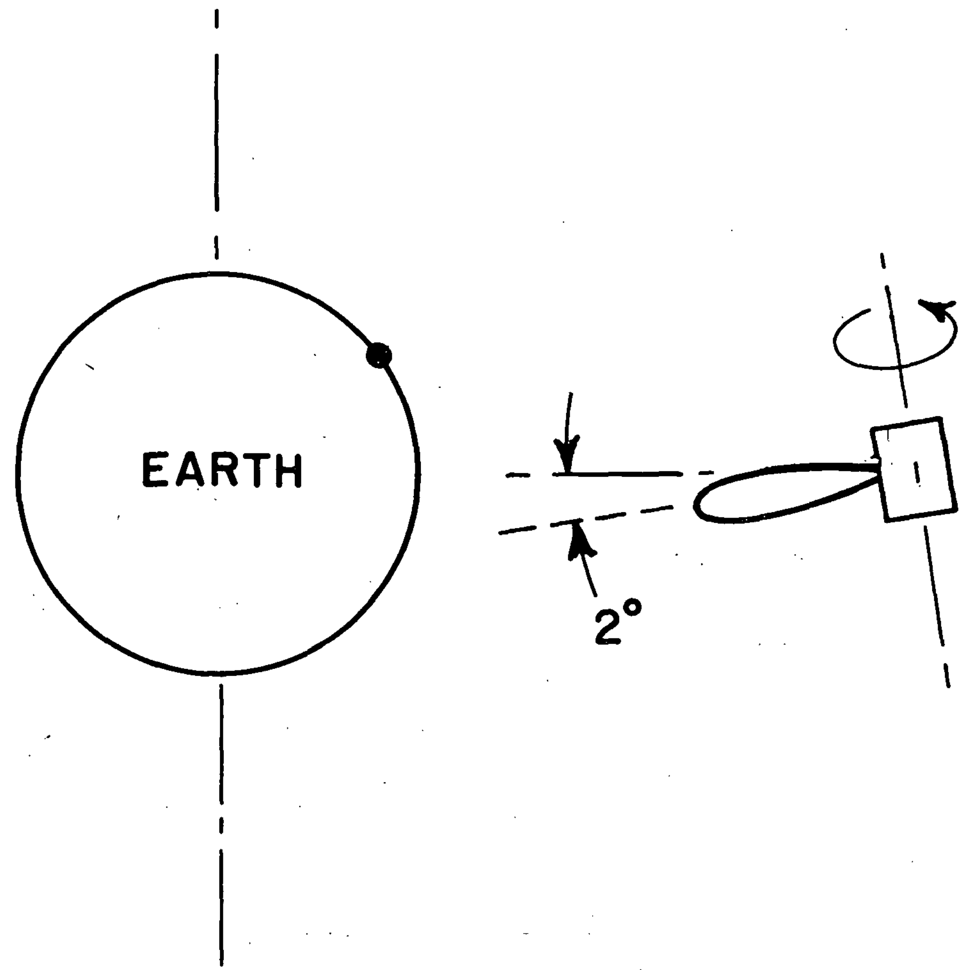

Fig. 2b. Spin modulation and its diurnal variation. (Scale distorted to exaggerate diurnal effects.) Maximum southward beam excursion.

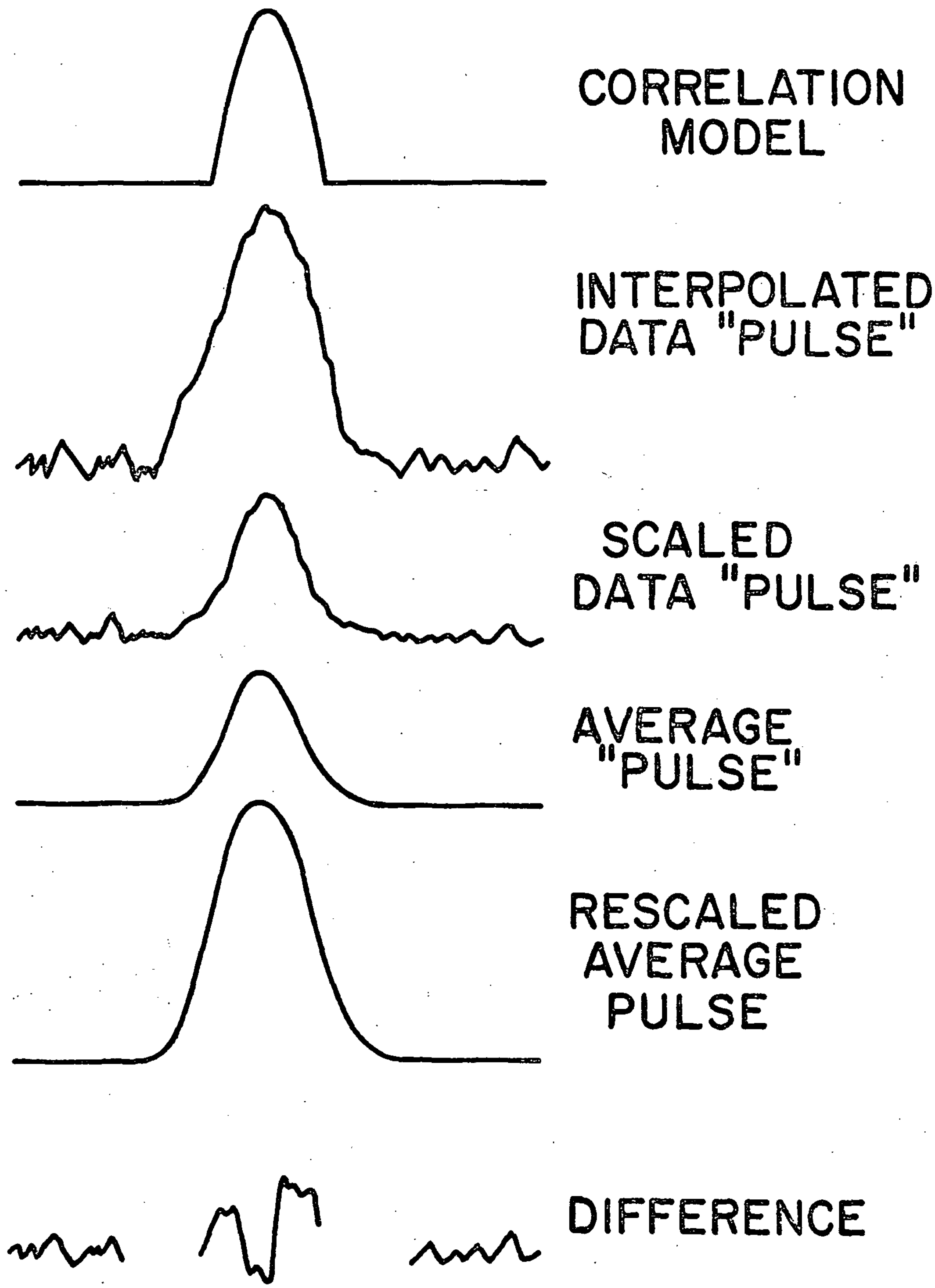

Fig. 3. Data analysis procedure.

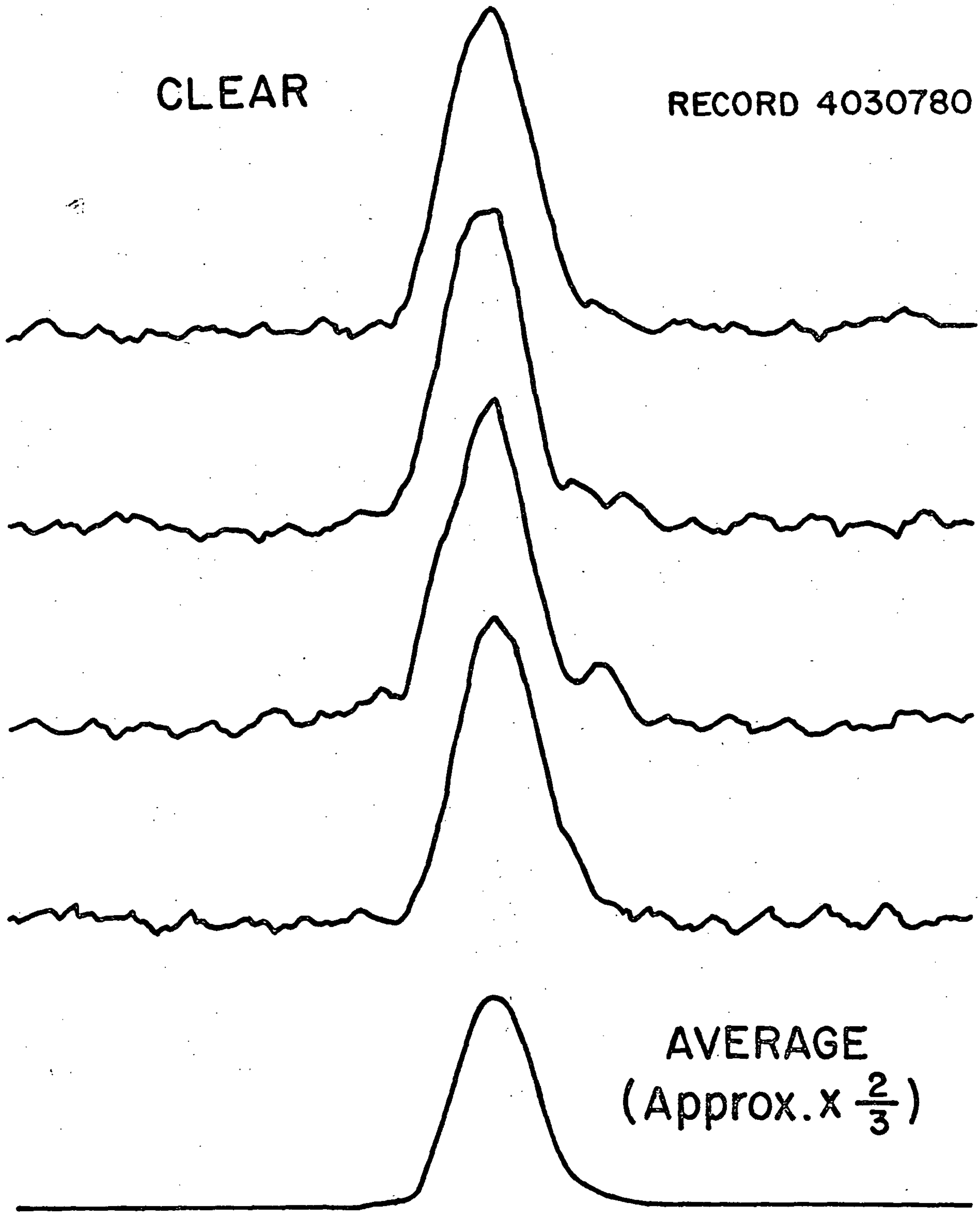

Fig. 4. Signal pulses and averaged pulse in correlated position. Clear sky.

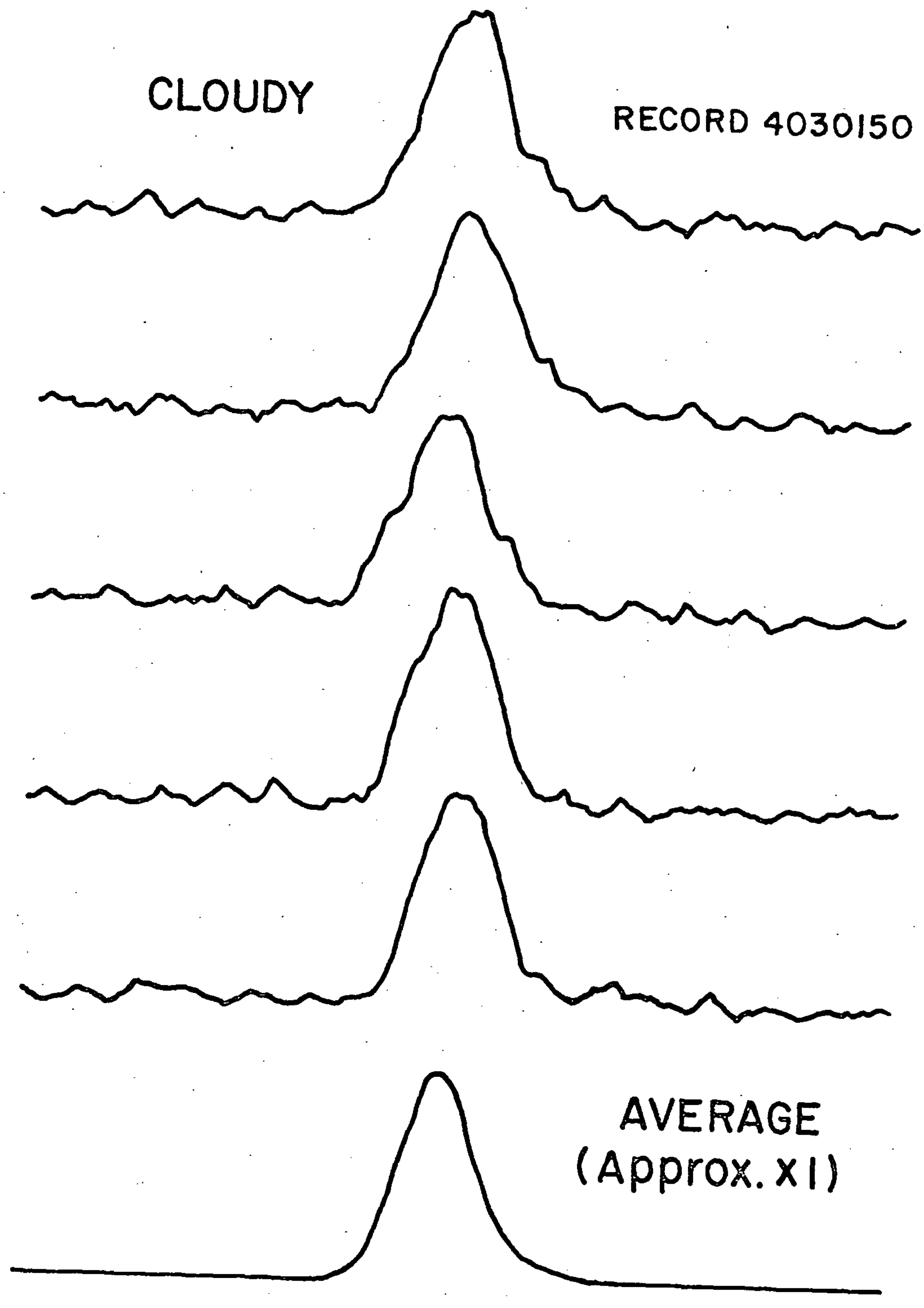

Fig. 5. Signal pulses and averaged pulse in correlated position. Cloudy sky.

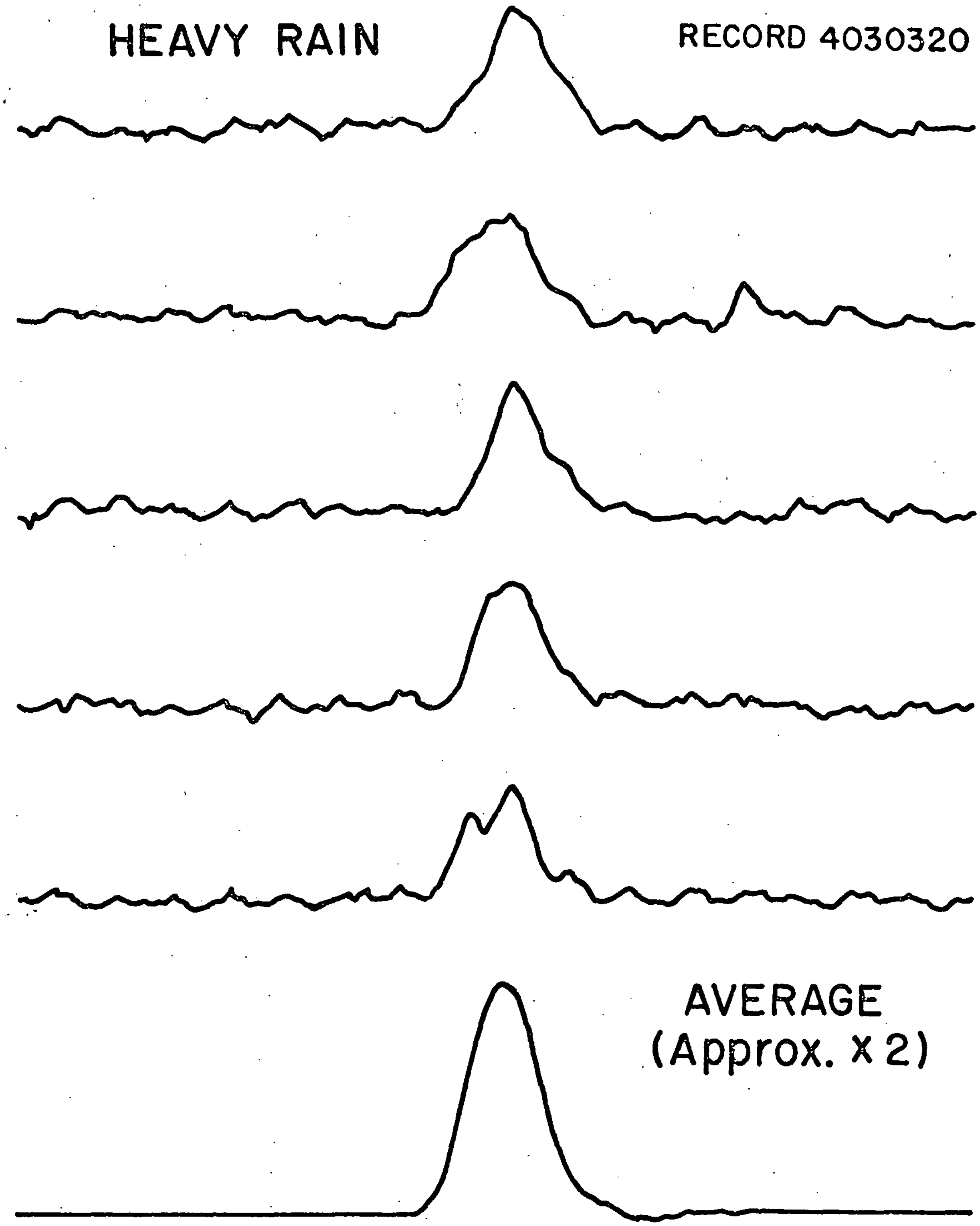

Fig. 6. Signal pulses and averaged pulse in correlated position. Hard rain.

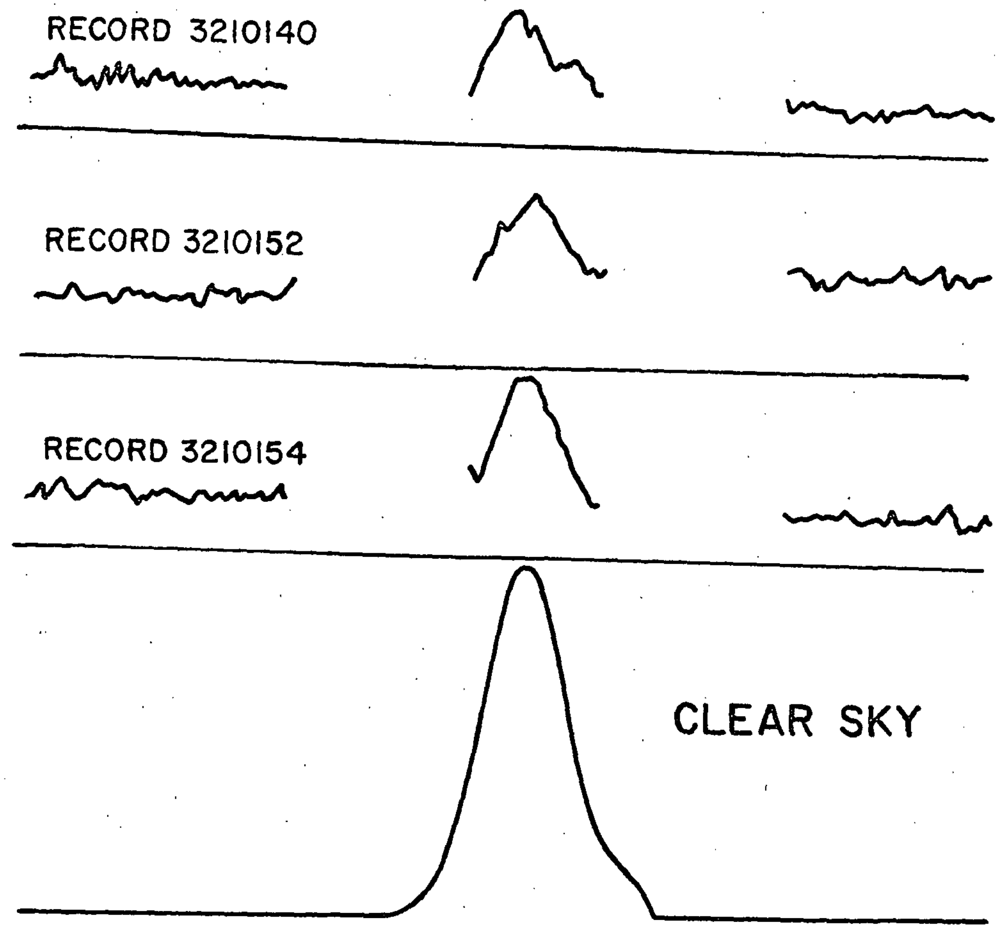

Fig. 7. Correlation of rms signal plus noise with average signal strength for 3 records, each containing approximately 40 pulses.

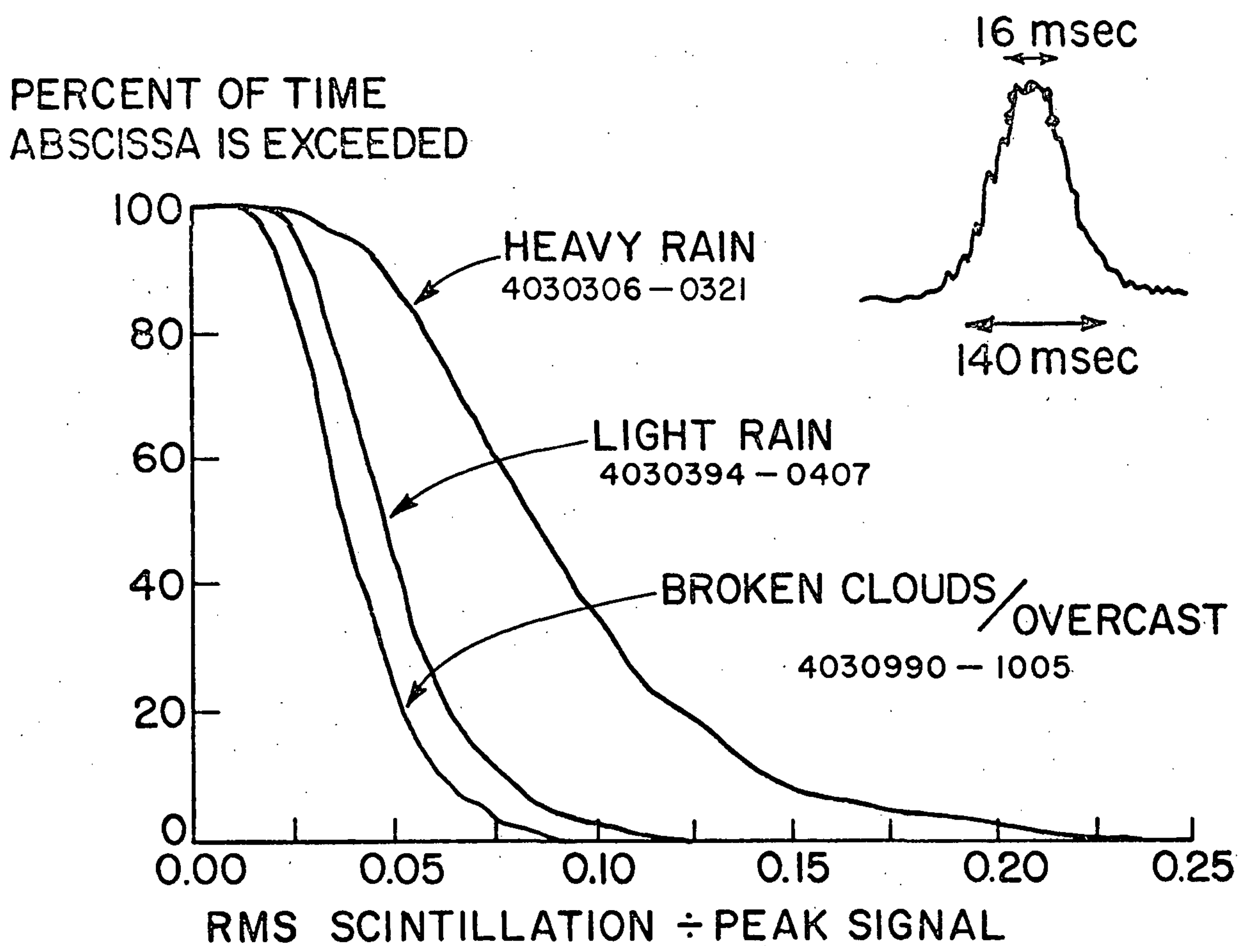

Fig. 8. Distribution of fast scintillations.

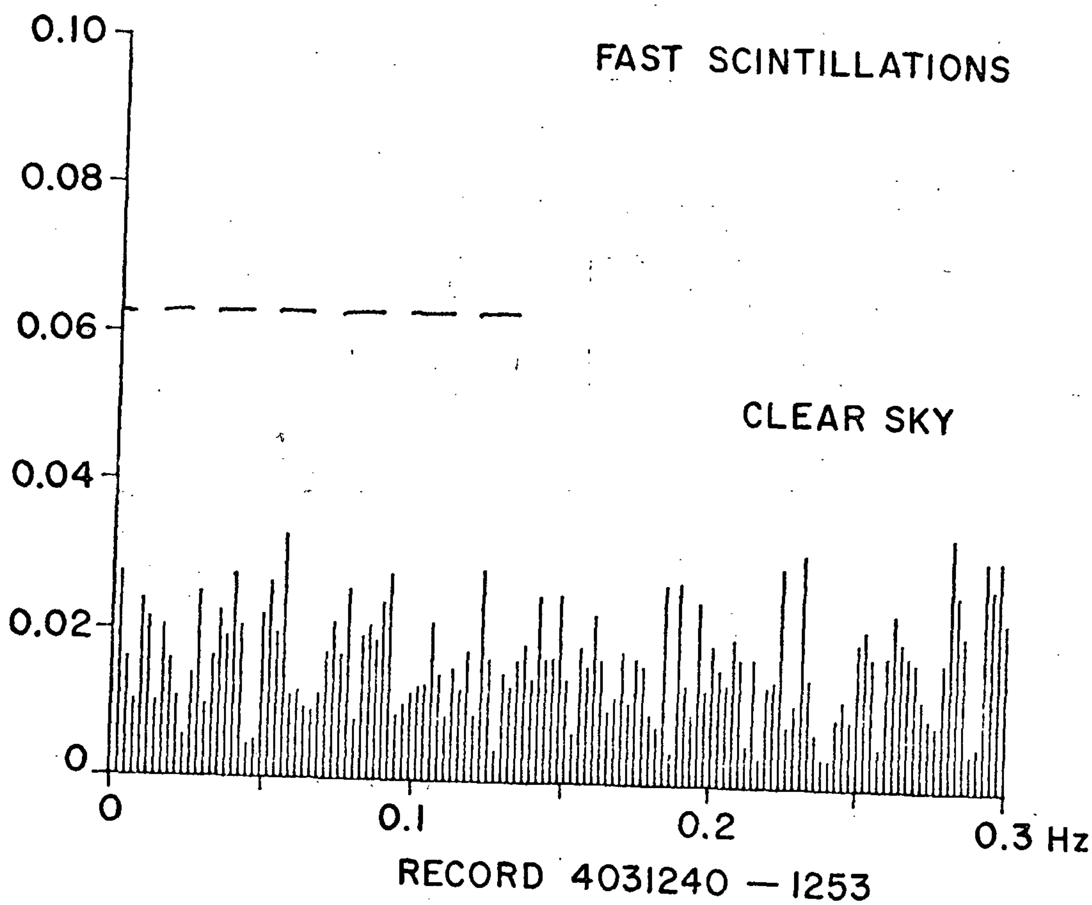

Fig. 9. Spectrum of fast scintillations. Clear sky.

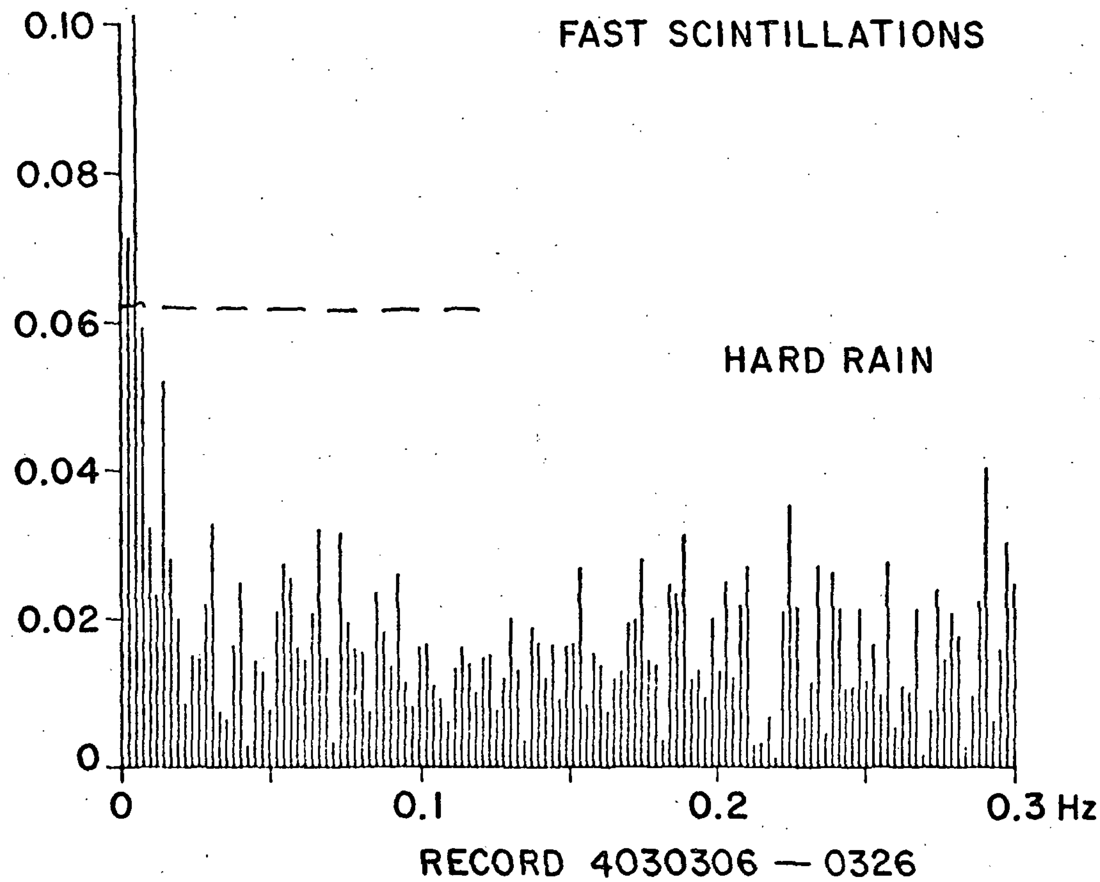

Fig. 10. Spectrum of fast scintillations. Hard rain.

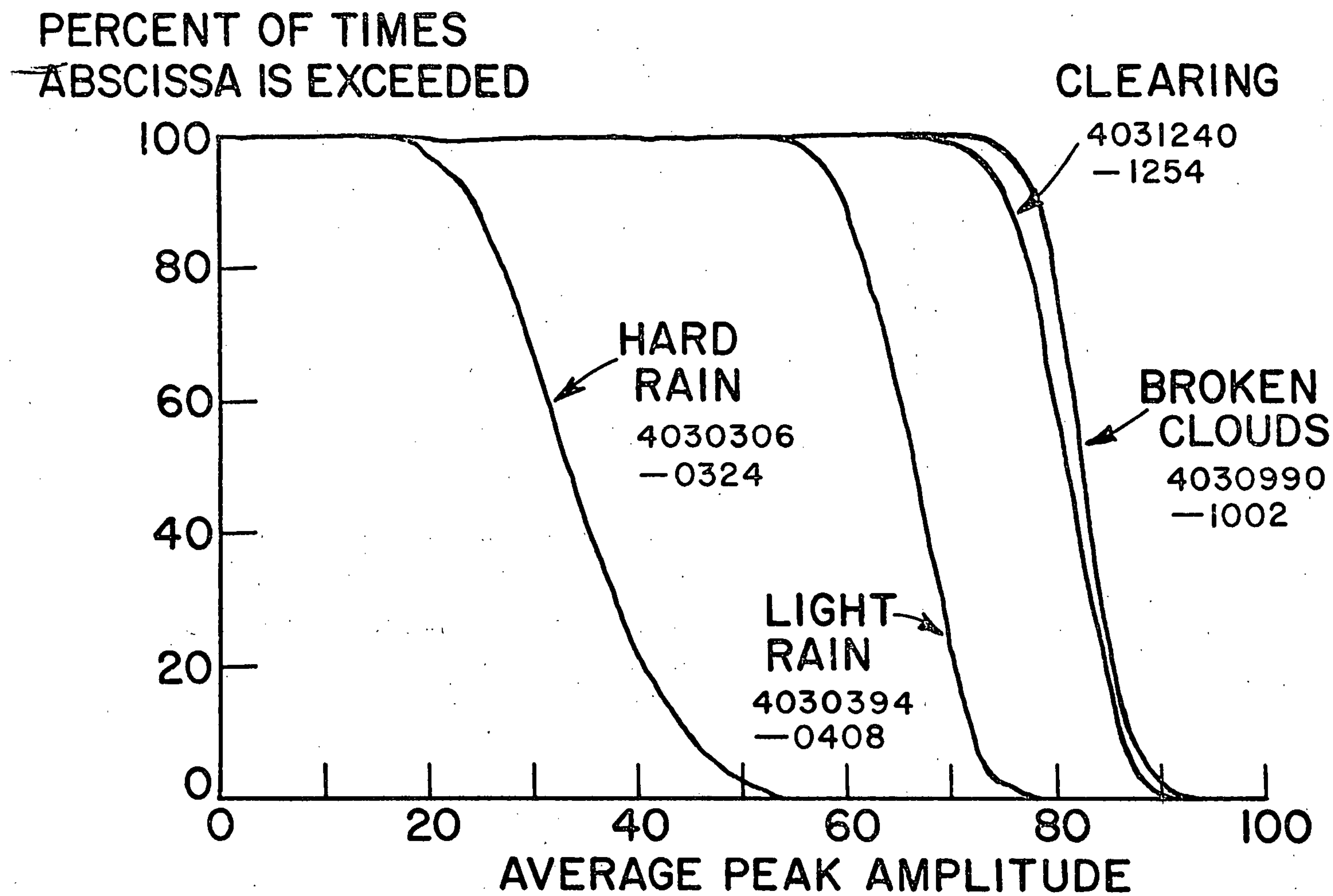

Fig. 11. Distribution of slow scintillations.

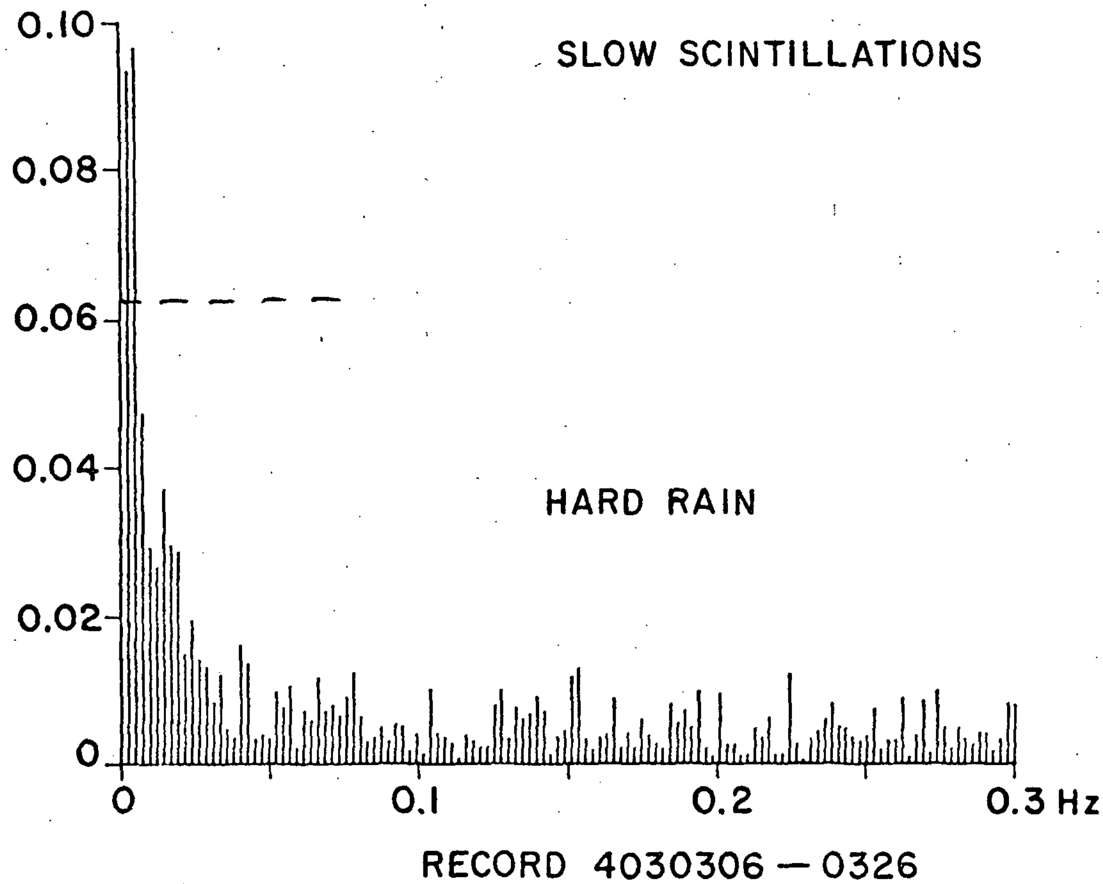

Fig. 12. Spectrum of slow scintillations. Hard rain.

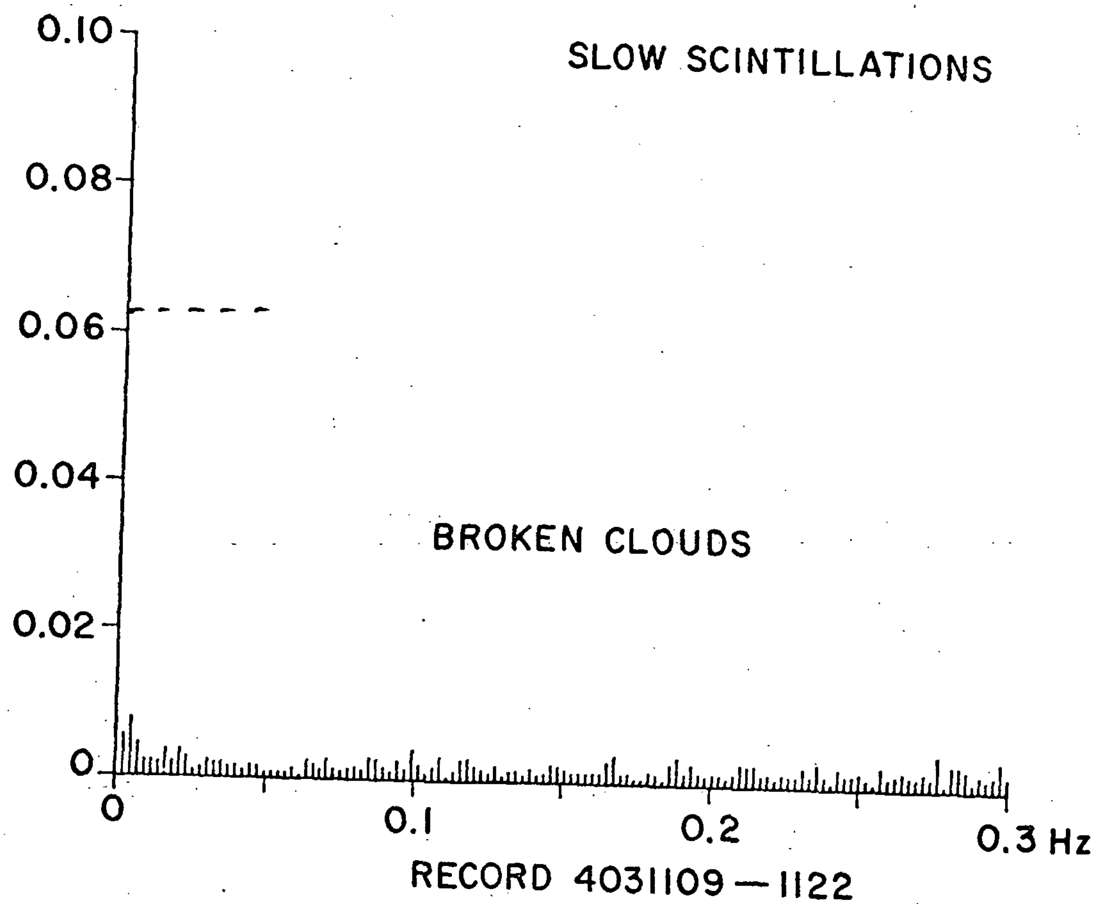

Fig. 13. Spectrum of slow scintillations. Broken clouds.

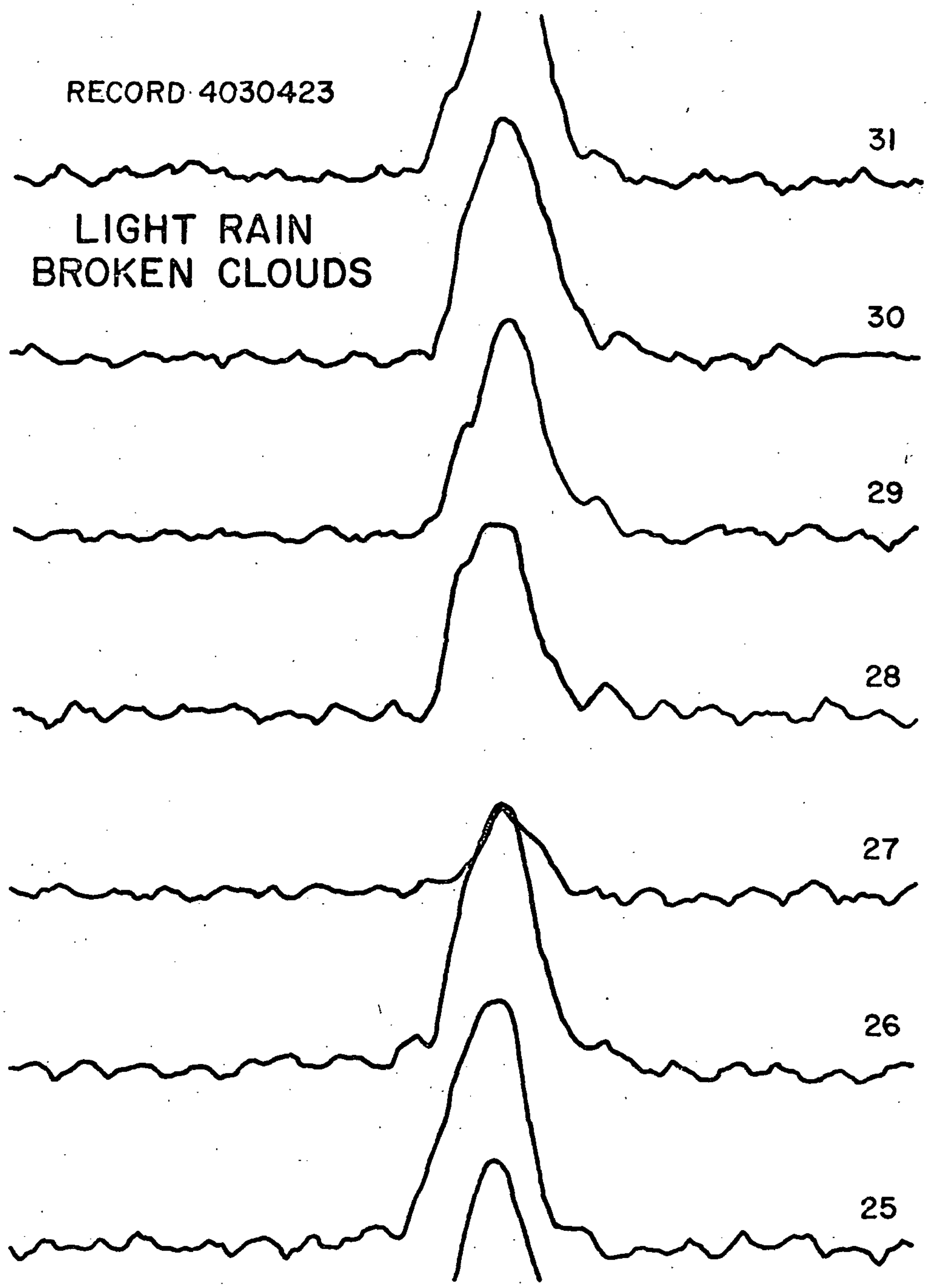

Fig. 14. Anomalous signal: Pulse 27 has significantly reduced amplitude.

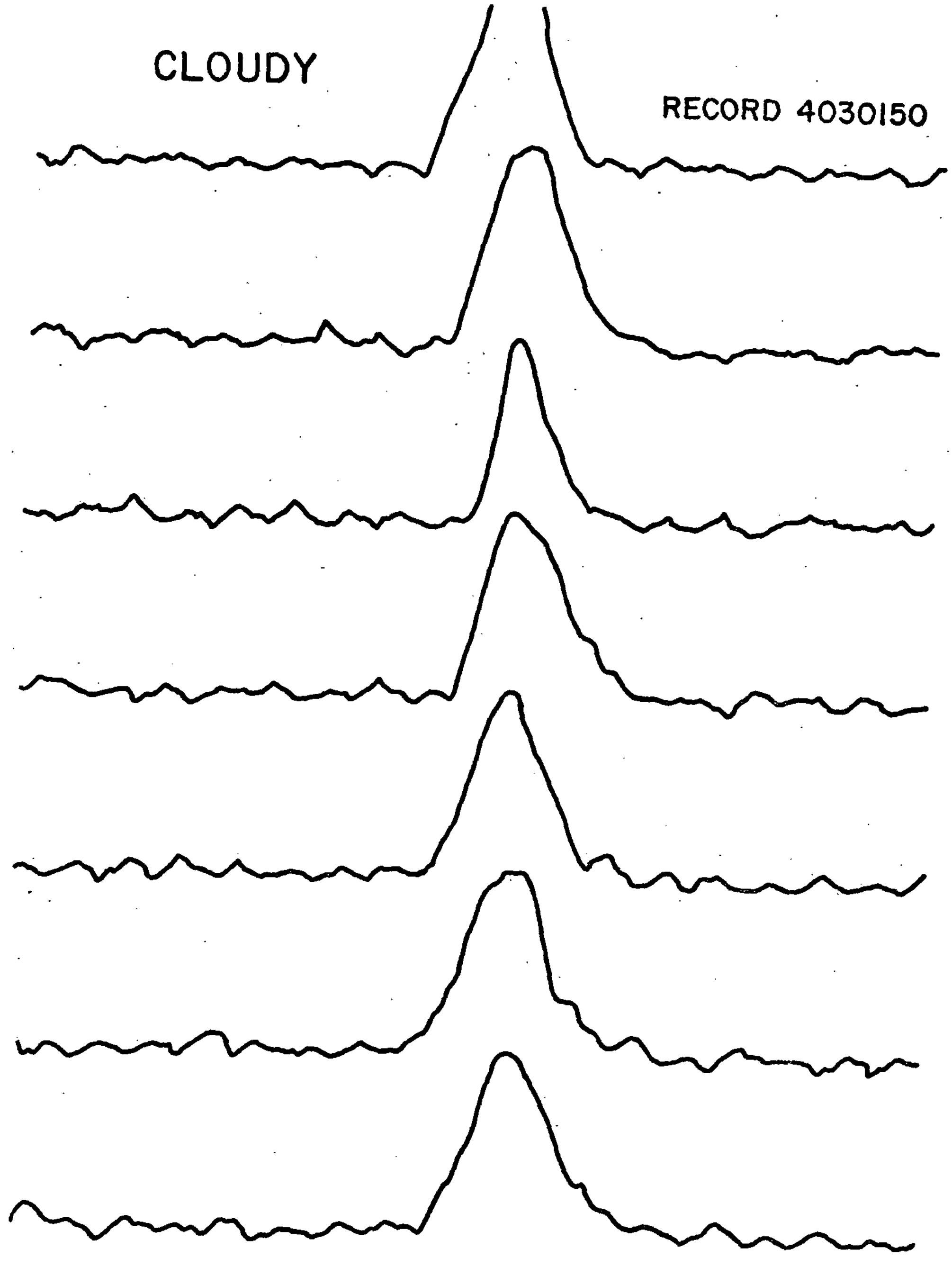

Fig. 15. Anomalous signal: fifth pulse from bottom has significantly reduced width.

TABLE A
Data digitized for scintillation analysis

Date(1)	Site(2)	Analog Tape No.	Length(3)	Analog Tape Speed Inches/Sec. Record	Analog Tape Speed Inches/Sec. Reproduce	Digital Tape No.	Weather Annotations(6)
5/19/71	214	38	3.0	1-7/8	3-3/4	1	Light rain, intermittent, overcast
4/15/71	213	16	1.0	1-7/8	3-3/4(4)	21	Broken sky (20-80% cloud cover)
6/26/70	214	27	2.0	1-7/8	3-3/4(4)	2	Showers, overcast, clearing
6/15/70	214	23	11.0	1-7/8	3-3/4	3	Cloudy, hard rain, light rain, overcast, clear
4/15/71	213	16	1.0	1-7/8	1-7/8	4	Broken sky (20-80% cloud cover)
6/17/70	213	6	6.0	1-7/8	3-3/4	5	Overcast, broken clouds, thunderstorm
7/06/70	213	9	11.0	1-7/8	3-3/4	6	Light clouds, wind 20 mph
6/21/71	214	41	3.0	1-7/8	3-3/4(4)	7A	Intermittent, overcast
6/29/71	214	42	2.0	1-7/8	3-3/4(4)	7B	Threatening, rain, drizzle
7/08/70	214	31	10.0	1-7/8	3-3/4(4)	8	Drizzle, rain, overcast, heavy rain
6/15/70	213	4	11.0	1-7/8	3-3/4	9	Rain, light rain, overcast, clearing, drizzle
6/13/71	214	40	6.0	1-7/8	3-3/4	10	Light rain, shower, overcast, broken-clouds
7/06/70	214	29	12.0	1-7/8	3-3/4	11(5)	Broken clouds, clear, haze - high humidity
6/14/70	213	3	5.0	1-7/8	3-3/4	12	Cloudy, rain, broken clouds, haze
7/17/70	214	30	12.0	1-7/8	3-3/4	13	Light thin clouds
7/06/70	214	29	12.0	1-7/8	3-3/4	14	Broken clouds, clear, haze, high humidity
6/25/70	214	26	4.0	1-7/8	3-3/4	15	Cloudy, light rain, clearing
7/06/70	214	28	11.28	1-7/8	3-3/4	16	Scattered clouds, clearing, cloudy
6/12/70	213	2	0.8	1-7/8	3-3/4	22	Cloudy

(1) Date of Observation
(2) 214 = mobile site, 213 = fixed site
(3) Length of time data was taken, in hours
(4) Tape speed 7-1/2 ips for calibrations
(5) Only 5 hours of data were digitized
(6) Annotations at time of observation

ACKNOWLEDGMENT

The contributions to the development of the interpolation, correlation, and averaging algorithms by Steven J. Struharik are gratefully acknowledged.

REFERENCES

[1] L. J. Ippolito, "Millimeter Wave Propagation Measurements from the Applications Technology Satellite ATS-5," IEEE Trans. on Antennas and Propagation, v. AP-18, No. 4, pp. 535-552, July 1970.

[2] D. B. Hodge, "A 15.3 GHz Satellite-to-Ground Diversity Experiment Utilizing the ATS-5 Satellite," Radio Science, v. 9, No. 1, pp. 1-6, January 1974.

[3] D. B. Hodge, "Path Diversity for Reception of Satellite Signals," J. de Recherches Atmospheriques, v. 9, No. 1-2, June 1974.

[4] L. J. Ippolito (Ed.), Earth Satellite Propagation Above 10 GHz, Report X-751-72-208, NASA Goddard Space Flight Center, May 1972.

[5] L. J. Ippolito (Ed. and contributor), Millimeter-wave Propagation Experiments Utilizing the ATS-5 Satellite, Report X-751-70-428, NASA Goddard Space Flight Center, November 1970.

[6] Ibid, pp. 1-4 and 1-5.

[7] S. J. Struharik and C. A. Levis, "Digital Averaging of Millimeter Wave Signals from the ATSE Satellite for Scintillation Analysis", The Ohio State University ElectroScience Laboratory, September 1972.

APPENDIX - DATA IDENTIFICATION

The following scheme for identifying data is used in this report. Data are grouped in records, each representing 8192 sampled data points occupying approximately 31 seconds in real time. Each such record is identified by a 7-digit number. The first digit designates the receiving terminal at which the data was recorded; 3 designates station 213, a stationary terminal, while 4 designates station 214, a transportable terminal located 4 kilometers from the fixed site prior to 1971 and 8 km from the fixed site during and after 1971. The location is 40°00'N and 83°02'W and the elevation angle to the satellite was approximately 39°. Further details of the station configurations are given in references 2 and 5. The second and third digits in the record identification designate a digital tape, as specified in Table A. The final four digits specify the position of the record within the digital tape. Thus the record identification 4030308-0321, as given in Fig. 8 for "heavy rain", indicates that the data was taken at the mobile terminal, was transcribed to digital tape 3 (which, from Table A, can be seen to have been originally observed and recorded on 15 June 1970), and represents approximately 7.2 minutes (14 x 31 seconds) of data.